

# Dynamics of atom-atom correlations in the Fermi problem

Massimo Borrelli<sup>1</sup>, Carlos Sabín<sup>2</sup>, Gerardo Adesso<sup>3</sup>, Francesco Plastina<sup>4,5</sup>, Sabrina Maniscalco<sup>1,6</sup>

<sup>1</sup>SUPA, EPS/Physics, Heriot-Watt University, Edinburgh, EH14 4AS, United Kingdom

<sup>2</sup>Instituto de Física Fundamental, CSIC, Serrano 113-B, 28006 Madrid, Spain

<sup>3</sup>School of Mathematical Sciences, The University of Nottingham, University Park, Nottingham NG7 2RD, United Kingdom

<sup>4</sup>Dipartimento di Fisica, Università della Calabria, 87036 Arcavacata di Rende (CS), Italy

<sup>5</sup>INFN-Gruppo Collegato di Cosenza, Italy

<sup>6</sup>Turku Center for Quantum Physics, Department of Physics and Astronomy, University of Turku, FIN20014, Turku, Finland

E-mail: mb325@hw.ac.uk

**Abstract.** We present a detailed perturbative study of the dynamics of several types of atom-atom correlations in the famous Fermi problem. This is an archetypal model to study micro-causality in the quantum domain where two atoms, the first initially excited and the second prepared in its ground state, interact with the vacuum electromagnetic field. The excitation can be transferred to the second atom via a flying photon and various kinds of quantum correlations between the two are generated during this process. Among these, prominent examples are given by entanglement, quantum discord and nonlocal correlations. It is the aim of this paper to analyze the role of the light cone in the emergence of such correlations.

## 1. Introduction

Since its original conception, the two-atom Fermi problem [1] has been the subject of an intense academic debate. Stated in very simple terms, this *gedanken* experiment goes as follows: suppose there are two two-level atoms (qubits), say  $A$  and  $B$ , spatially separated by a distance  $r$  and interacting independently with a the (multi-mode) quantized electromagnetic field, initially in the vacuum state. The atom  $A$  is in an excited state  $|e\rangle$  whereas the atom  $B$  is in its ground state  $|g\rangle$ . At some time  $t_0$  the atom  $A$  emits a photon. The original question by Fermi was then the following: as long as the two atoms are causally disconnected, is the excitation probability of  $B$  independent on the presence of  $A$ ? This question points at the very foundations of quantum mechanics: do quantum mechanical probabilities respect micro-causality? Over the past years a considerable amount of literature has dealt with this problem and several perturbative solutions have been proposed [2, 3, 4, 5, 6], sometimes even presenting opposite conclusions. Recently, in Ref.[7], a non-perturbative proof of strict causality in the Fermi problem has been finally given along with an explanation of

why the existence of correlations outside the light-cone connecting the two atoms is not in contrast with micro-causality. In fact, in a previous paper [8], some of the same authors had already studied the dynamics of concurrence [9] and found that it starts increasing just before  $(t - t_0) = r/c$  by a very tiny amount.

In this paper, motivated by such results, we take a step further and investigate the dynamics of other types of atom-atom correlations. In particular, besides extending the analysis of entanglement dynamics, we study the time evolution of geometric quantum discord and (classical) connected correlation functions. Quantum discord was first introduced by Ollivier and Zurek [10, 11] as a novel measure of the quantumness of correlations. The idea behind it is conceptually very simple. Quantum discord is indeed defined as the discrepancy, in the quantum regime, between two classically equivalent definitions of mutual information. It is believed to capture a more general type of quantum correlation than entanglement, in the sense that quantum states with zero entanglement but non-zero quantum discord do exist (see e.g. [12, 13, 14, 15, 16, 17]). Unfortunately, the computation of quantum discord implies solving a rather complicated minimization problem and, although considerable improvements have been made over the last years [18], analytical results are available for very few cases only [19, 20, 21]. In order to overcome such computational issues, alternative indicators of general quantum correlations have been recently introduced, mostly based on distance-based approaches [22, 23]. On the other hand, connected correlation functions provide a statistical quantifier of the (classical) correlations extractable during a joint measurement of the two atoms [24, 25, 26].

The results reported in this article have a double merit: on one hand they give a more complete picture of the dynamics of correlations in the two-atom Fermi problem. In fact, to the best of our knowledge, this is the first study of quantum discord and more general correlation dynamics in such a physical model, where an exact solution of the dynamics is still missing. As it turns out, all the types of correlations we consider have a nice physical interpretation in terms of a few relevant physical processes of the dynamics. On the other hand our results suggest a way to detect atom-atom correlations outside the light cone, that is, when the two atoms are causally disconnected. It is important to remark that our calculations are performed in the framework of time-dependent perturbation theory and they are exact and consistent up to the second order in the coupling constant. However, this is certainly not a problem since, as stated above, strict causality in the model has been analytically proven with no usage of perturbation theory [7]. Moreover, the time interval under scrutiny falls within the limits of validity of our approach provided the two atoms are not that distant.

## 2. The Model

We will consider a one-dimensional physical setup. A pair of two-level superconducting qubits (artificial atoms)  $A$  and  $B$ , separated by a fixed distance  $r$ , interact with an electromagnetic field propagating along the open transmission line connecting them. We name the atomic levels as  $\{|g\rangle, |e\rangle\}$  and we assume the following multimode structure for

the field

$$V(x) = \int dk \sqrt{N\omega_k} [e^{ikx} a_k + e^{-ikx} a_k^\dagger] \quad (1)$$

where  $N$  is a normalization factor which may accommodate different circuit QED architectures, the dispersion relation is linear  $\omega_k = v|k|$ , and  $a_k, a_k^\dagger$  are the usual annihilation and creation operator satisfying boson commutation relations  $[a_k, a_{k'}^\dagger] = \delta_{k,k'}$ . We define  $\Omega_J = \omega_{J_e} - \omega_{J_g}$  ( $J = A, B$ ) the energy separations between the qubit levels and we assume the qubits to be much smaller than the relevant wavelengths  $\lambda_J = v/(\Omega_J/(2\pi))$ ,  $v$  being the propagation velocity of the field quanta which in this scheme depends on the microscopic details of the model. Specifically,  $v = 1/\sqrt{cl}$ ,  $c$  and  $l$  being the capacitance and inductance per unit length respectively. A typical value is  $v = 1.2 \cdot 10^8 m/s$  [40]. Under these conditions the Hamiltonian,  $H = H_0 + H_I$ , splits into a free part for the qubits and the field

$$H_0 = \frac{1}{2} \hbar (\Omega_A \sigma_A^z + \Omega_B \sigma_B^z) + \int_{-\infty}^{\infty} dk \hbar \omega_k a_k^\dagger a_k \quad (2)$$

and a point-like interaction between them

$$H_I = - \sum_{J=A,B} d_J V(x_J) \sigma_J^x \quad (3)$$

Here  $x_J$  are the fixed positions of the atoms, and  $d_J \sigma_J^x$  comes from a dimensional reduction of the matter- radiation interaction hamiltonian with two-level atoms and the electromagnetic field. We will consider the following initial state

$$|\psi(0)\rangle = |eg0\rangle, \quad (4)$$

where only qubit  $A$  is excited, while  $B$  and the field remain in their ground and vacuum states, respectively. We use the formalism of perturbation theory up to the second order and beyond Rotating Wave Approximation [8] and trace over the field degrees of freedom to obtain the corresponding two-qubit reduced density matrix  $\rho_X$  evaluated at  $t$ . In the interaction picture with respect to the free Hamiltonian  $H_0$ , the system evolves during a lapse of time  $t$  into the state

$$|\psi(t)\rangle = \mathcal{T}[e^{-i \int_0^t dt' H_I(t')/\hbar}] |eg\rangle \otimes |0\rangle, \quad (5)$$

$\mathcal{T}$  being the time ordering operator. Up to second order in perturbation theory the final state can be written as

$$\begin{aligned} |\psi(t)\rangle = & [(1 + A) |eg\rangle + X |ge\rangle] \otimes |0\rangle + \\ & (U_A |gg\rangle + V_B |ee\rangle) \otimes |1\rangle \\ & + (F |eg\rangle + G |ge\rangle) \otimes |2\rangle + \mathcal{O}(d^3). \end{aligned} \quad (6)$$

The coefficients for the vacuum, single-photon, and two-photon states, are computed using the action ( $\alpha = A, B$ )

$$\mathcal{S}_\alpha^+ = -\frac{i}{\hbar} \int_0^t e^{i\Omega t'} \langle e_\alpha | d\sigma_\alpha^x | g_\alpha \rangle V(x_\alpha, t') dt' = -(\mathcal{S}_\alpha^-)^\dagger \quad (7)$$

among different photon number states  $|n\rangle, n = 0, 1, 2, \dots$ , being  $|n\rangle \langle n| = \frac{1}{n!} \int dk_1 \dots \int dk_n |k_1 \dots k_n\rangle \langle k_1 \dots k_n|$  and  $|k\rangle = a_k^\dagger |0\rangle$ . Among the various terms present here, the only one containing an effective coupling between  $A$  and  $B$  is

$$X = \langle 0 | T(\mathcal{S}_B^+ \mathcal{S}_A^-) | 0 \rangle. \quad (8)$$

This includes photon exchange only inside the light cone,  $vt > r$ , and vacuum fluctuations for all values of  $t$  and  $r$ , being  $r = x_B - x_A$  the distance between the qubits. The remaining terms are

$$\begin{aligned} A &= \frac{1}{2} \langle 0 | T(\mathcal{S}_A^+ \mathcal{S}_A^- + \mathcal{S}_B^- \mathcal{S}_B^+) | 0 \rangle \\ U_A &= \langle 1 | \mathcal{S}_A^- | 0 \rangle, V_B = \langle 1 | \mathcal{S}_B^+ | 0 \rangle, \\ F &= \frac{1}{2} \langle 2 | T(\mathcal{S}_A^+ \mathcal{S}_A^- + \mathcal{S}_B^- \mathcal{S}_B^+) | 0 \rangle, G = \langle 2 | T(\mathcal{S}_B^+ \mathcal{S}_A^-) | 0 \rangle. \end{aligned} \quad (9)$$

Here,  $A$  describes intra-qubit radiative corrections, while  $U_A, V_B, F$  and  $G$  correspond to single-photon emission events by one or more qubits. The coefficients in Eq. (6) will be computed analytically as a function of two dimensionless parameters,  $\xi$  and  $K$ . The first one,  $\xi = vt/r$ , is a dimensionless time variable; the time  $\xi = 1$  corresponds to the light-cone, which separates two different spacetime regions, before and after photons can be exchanged. The second parameter is a dimensionless coupling strength

$$K = \frac{4d^2 N}{\hbar^2 v} = 2 \left( \frac{g}{\Omega} \right)^2. \quad (10)$$

Note that the qubit-line coupling  $g = d\sqrt{N\Omega}/\hbar$  corresponds to the qubit-cavity coupling that appears by taking the same transmission line and cutting it in order to have a length  $L = \lambda$  (thus creating a resonator). This formulation has the advantage of being valid both for inductive and capacitive coupling, the details being hidden in the actual expressions for  $d$  and  $N$ . Tracing over the states of the field, we arrive at the following reduced density matrix

$$\rho_X = \frac{1}{c} \begin{pmatrix} \rho_{11} & 0 & 0 & \rho_{14} \\ 0 & \rho_{22} & \rho_{23} & 0 \\ 0 & \rho_{23}^* & \rho_{33} & 0 \\ \rho_{14}^* & 0 & 0 & \rho_{44} \end{pmatrix}, \quad (11)$$

representing the two-qubit state in the basis formed by  $|ee\rangle$ ,  $|eg\rangle$ ,  $|ge\rangle$ , and  $|gg\rangle$ . The coefficients with the leading order of neglected contributions are

$$\begin{aligned} \rho_{11} &= |V_B|^2 + \mathcal{O}(d^4), \quad \rho_{22} = 1 + 2\text{Re}(A) + \mathcal{O}(d^4) \\ \rho_{33} &= |X|^2 + |G|^2 + \mathcal{O}(d^6), \quad \rho_{44} = |U_A|^2 + \mathcal{O}(d^4) \\ \rho_{14} &= U_A^* V_B + \mathcal{O}(d^4) = \langle 0 | \mathcal{S}_A^+ \mathcal{S}_B^+ | 0 \rangle + \mathcal{O}(d^4) \\ \rho_{23} &= X^* + \mathcal{O}(d^4), \end{aligned} \quad (12)$$

and the state is normalized,  $c = \sum_i \rho_{ii}$ .

### 3. Dynamics of Correlations

In this section we report our results regarding the dynamics of correlations between the two (artificial) atoms. We investigate the time evolution of the square root of geometric quantum discord  $\sqrt{D}$  [22], of the entanglement as measured by the negativity  $N$  [27], and of the maximum connected correlation function  $C$  [25] in the state  $\rho_X$ . We have chosen these three specific types of correlations (whose definitions and properties are reported below) for four reasons:

- (i) to best relate our results with the ones reported in [8] by using a different measure of entanglement;
- (ii) to have a more complete description of the time evolution of general quantum correlations;
- (iii) to compare quantum correlations with correlations having also a classical nature;
- (iv) to issue a comprehensive comparative analysis among *compatible* measures of different types of correlations.

The meaning of the latter point can be clarified in connection with our choice of using  $\sqrt{D}$ . One might in fact question why we are comparing different powers of geometric discord and entanglement. The reason for this is that we want to be consistent in the order of expansion of the perturbative analysis we have performed. A good test to check whether this is true is provided by a hierarchy-type relationship that exists between the three chosen quantities for arbitrary states  $\rho$  of two qubits, namely

$$C(\rho) \geq \sqrt{D}(\rho) \geq N(\rho). \quad (13)$$

The rightmost inequality in (13) was proven analytically in [16], while the leftmost one has been verified numerically in [28]. Notice that for pure two-qubit states both inequalities are saturated and (13) becomes a chain of equalities.

In our analysis, we have found no violation of the hierarchy (13) for any range of the relevant physical parameters characterizing the states  $\rho_X$ , which serves as a validating indication that our results are consistent up to the second order. As a general remark, we can conclusively state that all correlations whose time evolution we have looked at, start increasing before the time at which the two atoms become causally connected. However, the rate of increase changes a lot from one type of correlation to another.

Let us now introduce the measures of correlations of interest and then discuss the main aspects of their dynamical behavior. To this end, the Bloch representation of generic two-qubit states  $\rho$  will be useful [19]. Namely,

$$\begin{aligned} \rho &= \frac{1}{4} \sum_{i,j=0}^3 R_{ij} \sigma_i \otimes \sigma_j \\ &= \frac{1}{4} \left( \mathbf{I}_1 \otimes \mathbf{I}_2 + \sum_{i=1}^3 x_i \sigma_i \otimes \mathbf{I}_2 + \sum_{j=1}^3 y_j \mathbf{I}_1 \otimes \sigma_j + \sum_{i,j=1}^3 t_{ij} \sigma_i \otimes \sigma_j \right), \end{aligned} \quad (14)$$

where  $R_{ij} = \text{Tr}[\rho(\sigma_i \otimes \sigma_j)]$ ,  $\sigma_0 = \mathbf{I}$ ,  $\sigma_i$  ( $i = 1, 2, 3$ ) are the Pauli operators;  $\vec{x} = \{x_i\}$  and  $\vec{y} = \{y_i\}$  represent the three-dimensional Bloch column vectors associated to the qubits  $A$  and  $B$ , respectively; and  $t_{ij}$  are the elements of the  $3 \times 3$  correlation matrix  $T$ .

### 3.1. Geometric discord

The geometric measure of quantum discord was first introduced in [22] and further investigations for two-qubit systems have been reported in [29, 16, 30]. Given a general bipartite  $d_A \otimes d_B$  quantum state  $\rho$ , the (normalized) geometric discord is defined as

$$D(\rho) \doteq \frac{d_A}{d_A - 1} \min_{\chi \in \Omega_0} \|\rho - \chi\|_2^2 \quad (15)$$

where  $\chi$  is a so-called classical-quantum state belonging to the set of zero-discord states  $\Omega_0$ ,  $\chi = \sum_i p_i |i\rangle\langle i| \otimes \varrho_{iB}$  and  $\|P - Q\|_2^2 = \text{Tr}(P - Q)^2$  is the squared Hilbert-Schmidt distance between a pair of operators  $P, Q$ . We can look at geometric discord as the minimum disturbance that would be induced in the system after a projective measurement on one of the two parties (say  $A$  in the above definition) [29]. It is important to remark that its value is dependent on the choice of the party to be measured [31]. Although in principle this expression can be very complicated to evaluate explicitly as it involves a minimization problem over the set of zero-discord states, an analytical formula exists for the general two-qubit case [22, 29, 30]. In terms of the Bloch picture [Eq. (14)], one has

$$D(\rho) = 2\text{Tr}[S] - 2\lambda_{\max}(S),$$

where  $\lambda_{\max}$  stands for ‘maximum eigenvalue’, and the matrix  $S$  is defined as  $S = \frac{1}{4}(\vec{x}\vec{x}^T + TT^T)$ . The (square root of) geometric discord of  $\rho_X$  is then

$$\sqrt{D(\rho_X)} = \sqrt{[\text{Re}(U_A^* V_B)]^2 + |X|^2}. \quad (16)$$

The above formula is correct up to the second order and it has an immediate physical interpretation. The two terms in Eq.(16) come indeed from first and second order contributions to the time evolution of the state. In particular the  $X$  term accounts for photon-exchange between the two atoms and carries all the information available about causal propagation and atom state dressing. Interestingly, the processes which contribute to non-zero quantum discord are 0 and 1-photon processes and even though the (square root of) geometric quantum discord has a continuous evolution starting from  $t = 0$ , it is well sensitive to light-cone crossing, showing a peak at  $t = r/c$ .

### 3.2. Negativity

Negativity [27] is a well-known and easily computable measure of entanglement for bipartite systems which is based on the positivity of the partial transposition (PPT) criterion [35]. Given a general  $d \otimes d$  quantum bipartite state  $\rho$ , the (normalized) negativity is defined as

$$N(\rho) \doteq \frac{1}{d-1} \|\rho^{T_A} - \mathbf{I}_{AB}\|_1 \quad (17)$$

where the  $T_x$  refers to the partial transposition operation with respect to the  $x$  party ( $x = A, B$ ),  $\mathbf{I}_{AB}$  is the identity operator in the composed Hilbert space  $\mathcal{H}_A \otimes \mathcal{H}_B$  and  $\|M\|_1 = \text{Tr}|M| = \sum_i |m_i|$  is the trace norm for a matrix  $M$  with eigenvalues  $\{m_i\}$ . As in the case of geometric discord we can easily compute the negativity of  $\rho_X$  up to the second order in time-dependent perturbation theory and we obtain the following expression

$$N(\rho_X) = \max \left\{ 0, \sqrt{(|U_A|^2 - |V_B|^2)^2 + 4|X|^2} - |U_A|^2 - |V_B|^2 \right\}. \quad (18)$$

The three physical processes contributing to entanglement are exactly the same as for geometric discord. However, in this case there is a time-dependent condition for entanglement to start increasing. Indeed it is easy to check that as long as the following condition is fulfilled

$$\frac{|X|^2}{|U_A|^2 |V_B|^2} \leq 1 \quad (19)$$

entanglement will be zero. Intuitively, this means that for entanglement to be non-zero, second-order processes must dominate over first-order ones. It is worth noticing that such a kind of constraint is absent in the case of the (square root of) geometric discord, which amounts simply to the sum of two positive and continuous functions.

### 3.3. Maximum connected correlation function

Geometric discord and entanglement are quantities which are strictly connected to the quantum character of a system and, indeed, they miss a classical analogue. In this respect, they are key quantities when it comes to understanding the interplay between the foundations of quantum mechanics and micro-causality, one of the postulates of relativity theory. However, one might also be interested in correlations arising from observable quantities such as, for instance, angular momenta and in general spin-like operators. We thus study the atom-atom (classical) connected correlation functions [26], to reveal the highest level of sensitivity at which the Bloch vectors of the two atoms perceive each other outside and inside the light cone. Given a bipartite state  $\rho$  of a pair of two-level quantum systems, we define the maximum connected correlation function  $C(\rho)$  as follows

$$C(\rho) \doteq \max_{n,n'} \{ \langle (\vec{\sigma} \cdot \hat{n})_A \otimes (\vec{\sigma} \cdot \hat{n}')_B \rangle_\rho - \langle (\vec{\sigma} \cdot \hat{n})_A \rangle_\rho \langle (\vec{\sigma} \cdot \hat{n}')_B \rangle_\rho \} , \quad (20)$$

where  $\vec{\sigma}$  is the three-component Pauli-operator vector and  $(\vec{\sigma} \cdot \hat{n})$  is the projection of such a spin vector along the direction pointed by  $\hat{n}$ . For generic two-qubit states  $\rho$  decomposed in Bloch form as in Eq. (14), the maximum in Eq. (20) can be computed in closed form and reads [25, 28]

$$C(\rho) = \sqrt{\lambda_{\max}(W^T W)} ,$$

where  $W = T - \vec{x} \vec{y}^T$ . We have computed  $C(\rho)$  for the state  $\rho_X$  and obtained an exact expression up to the second order,

$$C(\rho_X) = \max \left\{ |U_A|^2 + |V_B|^2 + 2\text{Re}(A), 2(|X| + |L|) \right\} \quad (21)$$

where  $L = U_A^* V_B$ . Once again, in this case only 0 and 1-photon processes contribute to the above correlation function. Moreover, with  $C(\rho_X)$  being dependent on  $X$ , it shows sensitivity to the light-cone crossing.

### 3.4. Results and Discussion

In the following we analyze the time evolution of the above correlations and compare their behavior qualitatively and quantitatively. We remark that all of the above quantities depend on the three terms  $U_A$ ,  $V_B$  and  $X$ , while the maximum connected correlation function displays an  $A$ -dependence as well. Fig.1(a) shows the behavior of the square root of geometric discord  $\sqrt{D(\rho_X)}$  as a function of the re-scaled time  $\xi = rt/v$  for different choices of the atom-field coupling constant, spanning from a weak to a strong coupling regime, and for a fixed distance  $r = v\pi/4\Omega$  between the qubits.

The first feature we notice, which is perhaps the most interesting one, is the relatively slow but continuous increase that the (square root of) geometric discord shows prior to the

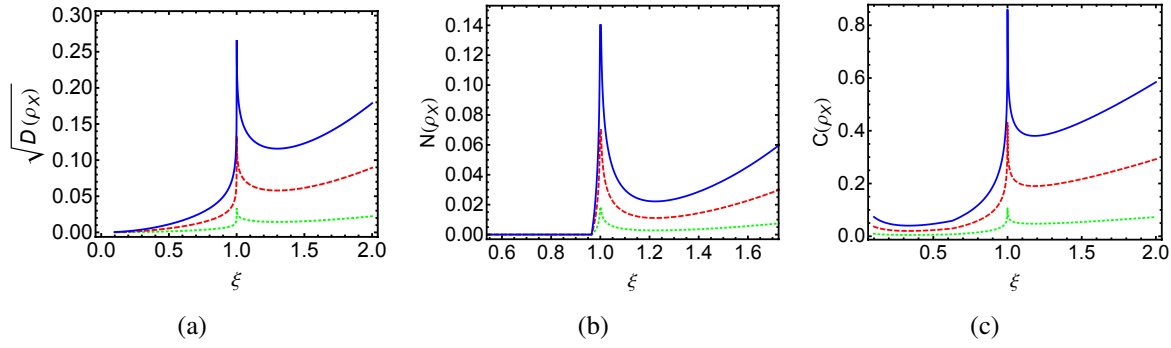


**Figure 1.** (Color online) Time-evolution of (a) the square root of geometric quantum discord  $\sqrt{D(\rho_X)}$ , (b) the negativity  $N(\rho_X)$  and (c) the maximum connected correlation function  $C(\rho_X)$ , for  $r = \nu\pi/4\Omega$  and three different choices of the coupling strength:  $Z = 50$  (dotted green),  $Z = 200$  (dashed red),  $Z = 400$  (continuous blue).

light-cone crossing. A similar behavior had been previously found by one of the present authors in [8] when studying the time evolution of entanglement measured by the concurrence [9] in the same model. However, unlike concurrence which started increasing within a very short time interval just before  $\xi = 1$ , the (square root of) geometric discord reaches finite values for a much longer time interval inside the space-like region  $J_S \equiv \{0 \leq \xi \leq 1\}$ . If we recall the interpretation of geometric discord mentioned above, we may argue that a one-party measurement performed at any time inside  $J_S$  will always induce a disturbance on the composite system.

Secondly, we observe a peak at  $\xi = 1$  which is independent of the interaction regime. The height of such a peak, and more generally the global magnitude of the (square root of) geometric discord, increases as we increase the coupling. These latter features are easily understood by looking at Eq.(16). As we said above the (square root of) geometric discord is the sum of a first order term, which does not carry any causality-related information, and a second order term, which instead does carry that kind of information. Hence, the stronger the interaction is, the bigger this second order term becomes.

In Fig.1(b) we show the time evolution of the negativity for the same three choices of coupling strengths and the same atom-atom separation. In this case we find essentially the same behavior as reported in [8] for concurrence. By comparing Fig.1(a) and 1(b), we may conclude that quantum discord is more sensitive to vacuum fluctuations, which are responsible for creating correlations between the two atoms outside the light cone. This behavior is well understood again when one looks at Eq.(16). The proportionality to  $X$ , which is a second-order 0-photon term, incorporates exactly this kind of trait.

Fig.1(c) shows the time evolution of the maximum connected correlation function  $C(\rho_X)$  for the same choice of parameters as in the previous plots. In this case we find something very interesting and not at all easily predictable. Indeed, like geometric discord, the maximum connected correlation function starts increasing significantly inside  $J_S$  and it shows a peak at  $\xi = 1$ . The maximum connected correlation function  $C(\rho)$  is not *a priori* a fully quantum



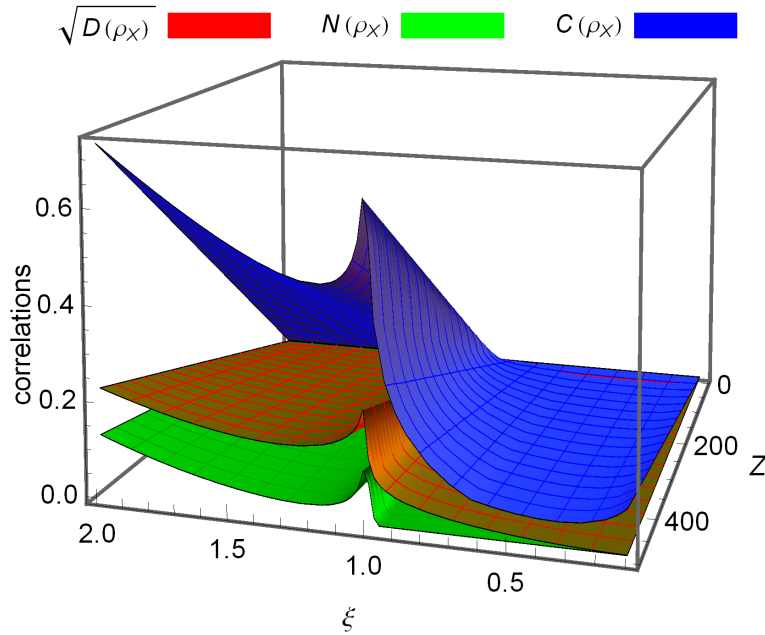


**Figure 2.** (Color online) Comparative plot displaying the maximum connected correlation function  $C$  (topmost surface, blue online), the square root  $\sqrt{D}$  of the geometric discord (middle surface, red online), and the negativity  $N$  (bottommost surface, green online), calculated for the state  $\rho_X$  as functions of the dimensionless time  $\xi$  and of the coupling strength  $Z$ , for  $r = v\pi/4\Omega$ .

quantity, and it determines how, on average, the Bloch vectors of the two atoms influence each other. The present results seem to suggest that this might be the key quantity to measure when it comes to an experimental detection of the dynamics of correlations, provided that a simultaneous set of optimal measurements on the two qubits can be efficiently performed in the laboratory frame.

It is worth noticing here that the optimal “measurement directions”  $\hat{n}, \hat{n}'$  are completely different in the space-like region  $J_S$  and on the light cone. Indeed, for  $\xi < 1$ , the correlation between the two Bloch vectors is best highlighted by measuring the effective spin projections in the equatorial  $x - y$  plane. On the light cone, on the other hand, the best choice is to measure  $\sigma_z$  for both qubits. This appears to be related to the fact that no excitation can reach the atom  $B$  before  $\xi = 1$  and that, as demonstrated in [8], it is only after this time that the excited state population of atom  $B$  starts depending on the presence of atom  $A$ . The vacuum fluctuations, thus, are able to correlate essentially transversal observables for  $\xi < 1$ , while for a longitudinal ( $z - z$ ) correlation, one has to wait the arrival of the light signal. Finally, in Fig. 2 reports a visual comparison of all the three indicators of correlations considered in the present analysis, as functions of  $Z$  and  $\xi$ . As anticipated, there is no violation of the general hierarchy (13), thus confirming that the perturbative analysis we have performed is consistent up to the present expansion order.

#### 4. Non-locality

One may wonder what the above results mean in term of non-locality. In this respect, a key quantity to investigate non-local effects in the dynamics of two two-level systems is the Bell parameter [36], resulting from well-known inequalities that local classical hidden variable theories cannot violate. To make a long story short, one identifies a set of joint measurements to be performed on the composite system. Then, based on the outcomes of such measurements, it is possible to define a statistical parameter  $\mathcal{B}$  for which a classical threshold value  $\mathcal{B}_C$  exists. Whenever the inequality

$$\mathcal{B} < \mathcal{B}_C$$

is violated, the state of the system under scrutiny is not reproducible by means of local classical hidden variable theories. Unfortunately, the other way around is not true: some mixed entangled states exist that do not violate any Bell inequality [37]. In the case of two two-level system, it is well known that  $\mathcal{B}_C = 2$ , whereas the maximum violation allowed by quantum mechanics is given by the so-called Tsirelson bound,  $\mathcal{B}_{\max} = 2\sqrt{2}$ , which is saturated by maximally entangled states. Hence, if for a given bipartite quantum state  $\rho$  we find  $2 < \mathcal{B}(\rho) \leq \in\sqrt{\epsilon}$ , such a state is not classically reproducible. We have considered two different Bell parameters in the present analysis: the conventional CHSH one [38] and its optimized version for “X”-shaped states such as  $\rho_X$ , given in [39]. The former, for the states in Eq. (11), reads as follows (up to the second perturbative order)

$$\mathcal{B}_{CHSH}(\rho_X) = -\sqrt{2}(\rho_{11} + \rho_{44} - \rho_{22} - \rho_{33} + 2\text{Re}\rho_{23} + 2\text{Re}\rho_{14}), \quad (22)$$

whereas the latter is [39]

$$\mathcal{B}_{OPT}(\rho_X) = 2\sqrt{u_1 + \max[u_2, u_3]}, \quad (23)$$

where

$$\begin{aligned} u_1 &= 4(|\rho_{14}| + |\rho_{23}|)^2 & u_3 &= 4(|\rho_{14}| - |\rho_{23}|)^2 \\ u_2 &= (\rho_{11} + \rho_{44} - \rho_{22} - \rho_{33})^2. \end{aligned}$$

The above quantities correspond to two different choices of the Bell parameters, that is, different choices of the angles along which we project the effective spin operators in a joint-measurement experiment. The main difference between them is that  $\mathcal{B}_{OPT}$  is optimal in the sense that it maximizes the violation of the related Bell inequality, whenever such a violation is present. We report in Fig.3(a) the time evolution of the the Bell parameter  $\mathcal{B}_{CHSH}$ . It is clear from these plots that, in order to observe a violation of the Bell inequality, a very strong coupling is required ( $Z \approx 1000$ ). However, such a violation is witnessed only in the surroundings of the light cone crossing  $\xi = 1$ . Fig.3(b) shows, instead, the time evolution of  $\mathcal{B}_{OPT}$ . Some qualitative and quantitative differences between these quantities, especially for  $\xi > 1$  and very strong coupling, are present. First of all we notice that, as expected, the optimized Bell parameter  $\mathcal{B}_{OPT}$  is greater than  $\mathcal{B}_{CHSH}$  for all couplings and times. Secondly, the latter is clearly more sensitive to the strong-coupling regime. This result makes perfectly sense if we look at the entanglement dynamics as a function of the coupling constant: the

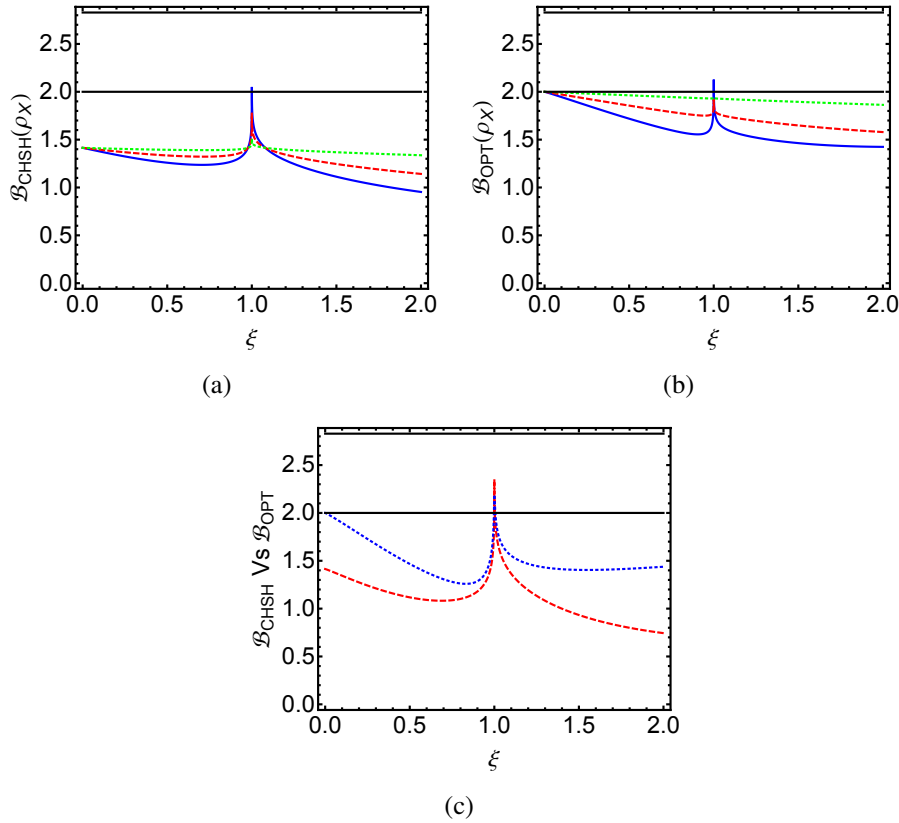


**Figure 3.** (Color online) (a) Bell-CHSH parameter  $\mathcal{B}_{CHSH}$  and (b) its optimized version  $\mathcal{B}_{OPT}$ , plotted for  $Z = 100$  (dotted green),  $Z = 400$  (dashed red) and  $Z = 800$  (continuous blue), as a function of  $\xi$ . The straight line at  $\mathcal{B} = 2$  gives the limit for a local realistic description. As one can see, in both cases, a very strong coupling is needed in order to have a clear violation of the inequality, occurring, however, only very close to the light cone crossing point. (c) Comparison between  $\mathcal{B}_{CHSH}$  (red dashed) and  $\mathcal{B}_{OPT}$  (blue dotted) for strong coupling  $Z = 1000$ . In all these plots  $r = v\pi/4\Omega$ .

bigger  $Z$  is, the more entanglement is present in the system, pushing up the Bell parameters' value. These last two features are best enlightened in the third plot 3(c) where the dynamics of the two Bell parameters we considered, is compared in the case of very strong coupling  $Z = 1000$ .

## 5. Experimental implementation

Now we will focus on the particular experimental set-up that we propose to test the results above. Clearly, we need the ability of fast on-off switching of the qubit-field interaction. We should be able to prepare the initial state Eq. (4) and let the interaction be active only during a finite time. We can conceive several circuit QED schemes in order to achieve these goals. As commented before our general formalism can accommodate several architectures; in particular, it is valid both for inductive and capacitive couplings. We can choose for instance a pair of three-junction flux qubits galvanically coupled to the center conductor of an open

transmission line. In Ref. [7] it is shown how the desired initial state can be prepared with high fidelity by varying an external magnetic flux adiabatically for qubit  $B$  and non-adiabatically for qubit  $A$ . After that, the interaction has to be switched on and kept constant during a given time interval. In Ref. [41] several modifications of the three-junction scheme are proposed in order to achieve couplings tunable in strength up to the ultra-strong regime. In particular, a specific set-up featuring an intermediate superconducting loop has been described in details in Ref. [42], where an effective interaction Hamiltonian between a qubit and a transmission line has been derived, that reads

$$H_I \propto \cos(f)\sigma_x V(x), \quad (24)$$

$f$  being related with an external magnetic flux  $\Phi$  threading the SQUID:  $f = 2\pi\Phi/\Phi_0$  (where  $\Phi_0 = h/2e$  is the flux unit). By a suitable modulation of the flux  $\Phi$ , thus, the interaction can be activated and switched off at will. State of the art circuit-QED technology allows variations of the magnetic flux at frequencies of about 10 GHz [40] and larger values are expected for the future [43]. As a result, switching times of the order of 0.1 ns and even shorter can be safely considered. Taking the values that we have considered in our plots, and typical circuit-QED parameters, such as  $v = 1.2 \cdot 10^8$  m/s and  $\Omega = 10^9$  m/s, the point  $\xi = 1$  is equivalent to an interaction time  $t \simeq 1$  ns. Thus, the region around  $\xi = 1$  is well within experimental reach. In particular the strongest value that we considered for the adimensional coupling  $Z$  is equivalent to  $g/\Omega \simeq 0.3$ , which is quite similar to the ones in cutting-edge experiments investigating the ultra-strong coupling regime [44, 45].

Once the interaction is switched off, quantum state tomography [46] may be performed in order to quantify the degree of correlations, using for instance the magnitudes that we have considered in this work. The dynamics is effectively frozen and the system remains in the state  $\rho_X(t)$ , so measurements can take as much time as required. In particular, it would be interesting to run the experiment for different interaction times inside and outside the light cone, in order to test both the peak at  $\xi = 1$  and the correlations for  $\xi < 1$ .

## 6. Concluding Remarks

To summarize, using second order perturbation theory we have discussed the dynamics of quantum correlations in the Fermi problem, which can be experimentally tested in a one-dimensional set-up involving two artificial atoms coupled to the electromagnetic field of an open ended transmission line. We have compared the time behavior of the entanglement, as measured by the negativity, and of more general quantum correlations such as the (square root of) geometric discord, and the maximum connected correlation function. All of these correlations display a peak at the light cone crossing point,  $\xi = 1$ , which corresponds to the time at which a signal from atom  $A$  arrives at  $B$ . The geometric discord and the connected correlation, however, have a substantially non-zero value also in the space-like region. This is due to the fact that electromagnetic vacuum fluctuations can induce (transverse) correlations that are signalled by these functions. As the light-cone is crossed, these correlations change their character and become longitudinal as a result of the fact that

the excited state population of the second atom starts to depend on the presence of the first one. We have briefly investigated non-local effects in this model as encoded in possible violations of Bell inequalities. We have found that a violation can occur in the neighborhood of the light-cone crossing and only for strong couplings between the atoms and the propagating field. We believe that both geometric discord and maximum connected correlations, which are found to be sensitive to causal propagation, are suitable candidates for understanding and testing experimentally the role of micro-causality in the dynamics of quantum correlations.

## Acknowledgments

We acknowledge the University of Nottingham (ECRKA/2011), the U.K. EPSRC [Grants EP/J016349/1 and EP/J016314/1 (subcode RDF/BtG/0612b/31)], the Finnish Cultural Foundation [Science Workshop on Entanglement], and the Emil Aaltonen foundation [Non-Markovian Quantum Information] for financial support. GA thanks D Girolami and M Piani for discussions.

## References

- [1] Fermi E 1932 *Rev. Mod. Phys.* **4** 87
- [2] Biswas A K, Compagno G, Palma G M, Passante R and Persico F 1990 *Phys. Rev. A* **42** 4291
- [3] Hegerfeldt G C 1994 *Phys. Rev. Lett.* **72** 596
- [4] Buchholz D and Yngvason J 1994 *Phys. Rev. Lett.* **73** 613
- [5] Power E A and Thirunamachandran T 1997 *Phys. Rev. A* **56** 3395
- [6] Milonni P W, James D F V and Fearn H 1995 *Phys. Rev. A* **52** 1525
- [7] Sabín C, del Rey M, García-Ripoll J J and León J 2011 *Phys. Rev. Lett.* **107** 150402
- [8] Sabín C, García-Ripoll J J, Solano E and León J 2010 *Phys. Rev. B* **81** 184501
- [9] Hill S and Wootters W K 1997 *Phys. Rev. Lett.* **78** 5022
- [10] Ollivier H and Zurek W H 2001 *Phys. Rev. Lett.* **88** 017901
- [11] Henderson L and Vedral V 2001 *J. Phys. A* **34** 6899
- [12] Ferraro A, Aolita L, Cavalcanti D, Cucchietti F M and Acín A 2010 *Phys. Rev. A* **81** 052318
- [13] Piani M, Gharibian S, Adesso G, Calsamiglia J, Horodecki P and Winter A 2011 *Phys. Rev. Lett.* **106** 220403
- [14] Streltsov A, Kampermann H and Bruss D 2011 *Phys. Rev. Lett.* **106** 160401
- [15] Campbell S, Apollaro T J G, Di Franco C, Banchi L, Cuccoli A, Vaia R, Plastina F and Paternostro M 2011 *Phys. Rev. A* **84** 052316
- [16] Girolami D and Adesso G 2011 *Phys. Rev. A* **84** 052110
- [17] Piani M and Adesso G 2012 *Phys. Rev. A* **85** 040301(R)
- [18] Modi K, Brodutch A, Cable H, Paterek T and Vedral V 2011 *e-print* arXiv:1112.6238
- [19] Luo S 2008 *Phys. Rev. A* **77** 042303
- [20] Girolami D and Adesso G 2011 *Phys. Rev. A* **83** 052108
- [21] Adesso G and Datta A 2010 *Phys. Rev. Lett.* **105** 030501; Giorda P and Paris M G A 2010 *Phys. Rev. Lett.* **105** 020503
- [22] Dakić B, Brukner C and Vedral V 2010 *Phys. Rev. Lett.* **105** 190502
- [23] Modi K, Paterek T, Son W, Vedral V and Williamson M 2010 *Phys. Rev. Lett.* **104** 080501
- [24] Verstraete F, Popp M and Cirac J I 2004 *Phys. Rev. Lett.* **92** 027901
- [25] Popp M, Verstraete F, Martín-Delgado M A and Cirac J I 2005 *Phys. Rev. A* **71** 042306
- [26] Wolf M M, Verstraete F, Hastings M B and Cirac J I 2008 *Phys. Rev. Lett.* **100** 070502
- [27] Vidal G and Werner R F 2002 *Phys. Rev. A* **65** 032314

- [28] Adesso G (unpublished)
- [29] Luo S and Fu S 2010 *Phys. Rev. A* **82** 034302
- [30] Girolami D and Adesso G 2012 *Phys. Rev. Lett.* **108** 150403
- [31] The geometric discord  $D$  can increase under quantum operations on the party that is not measured [32, 33]; as such, it should be regarded just as an indicator of nonclassical correlations rather than as a proper measure. It constitutes nonetheless a valid lower bound to another *bona fide* distance-based measure of quantum correlations defined in terms of relative entropy [13, 23], and it enjoys a specific operational interpretation for two-qubit states [34].
- [32] Hu X, Fan H, Zhou D L and Liu W-M 2012 *e-print* arXiv:1203.6149
- [33] Piani M 2012 *e-print* arXiv:1206.0231
- [34] Dakić B *et al* 2012 *e-print* arXiv:1203.1629
- [35] Peres A 1996 *Phys. Rev. Lett.* **77** 1413; Horodecki R, Horodecki P and Horodecki M 1996 *Phys. Lett. A* **210** 377
- [36] Bell J S 1964 *Physics* **1** 195
- [37] Werner R F 1989 *Phys. Rev. A* **40** 4277
- [38] Clauser J F, Horne M A, Shimony A and Holt R A 1969 *Phys. Rev. Lett.* **23** 880
- [39] Bellomo B, Lo Franco R and Compagno G 2010 *Phys. Lett. A* **374** 3007
- [40] Wilson C M, Johansson G, Pourkabirian A, Johansson J R, Duty T, Nori F, and Delsing P 2011 *Nature* **479** 376
- [41] Peropadre B, Forn-Díaz P, Solano E and García-Ripoll J J 2010 *Phys. Rev. Lett.* **105** 023601
- [42] Sabín C, Peropadre B, del Rey M and Martín-Martínez E 2012 *e-print* arXiv:1202.1230
- [43] Romero G, Ballester D, Wang Y M, Scarani V and Solano E 2012 *Phys. Rev. Lett.* **108** 120501
- [44] Forn-Díaz P, Lisenfeld J, Marcos D, García-Ripoll J J, Solano E, Harmans C J P M and Mooij J E 2010 *Phys. Rev. Lett.* **105** 237001
- [45] Niemczyk T *et al* 2010 *Nature Phys.* **6** 772
- [46] Steffen M *et al* 2006 *Science* **313** 1423